A Framework for Combining Lateral and Longitudinal Acceleration to Assess Driving Styles Using Unsupervised Approach

Yuanfang Zhu, Meilan Jiang, Toshiyuki Yamamoto, Naikan Ding, Hiroko Shinkai, Hirofumi Aoki, Kan Shimazaki

***Abstract*—Driving style assessment plays an important role in intelligent transportation system (ITS) applications, such as driving feedback provision and usage-based insurance. Many previous studies used supervised algorithms to profile drivers. However, this cannot be applied to large-scale unlabeled driving data, which are increasingly prevalent in the ITS context. This paper proposes a framework that combines lateral and longitudinal accelerations to assess a driver's driving style using an unsupervised approach. The framework first detects risky acceleration maneuvers using a statistical method based on the G-G diagram that shows combinations of lateral and longitudinal accelerations. Hierarchical clustering was used to classify the average driving behavior of drivers into high-, medium-, and low-risk groups. Further, a unique Gaussian mixture model is trained for each driver to score their driving style and decompose risky acceleration maneuvers into several risk components. Finally, the spatio-temporal characteristics are extracted to provide implicit factors on the risky behavior of drivers. The proposed method was applied to a large-scale dataset obtained by in-vehicle data recorders. The results demonstrate the necessity to combine the two axes of acceleration for driver behavior assessment. The proposed method can model individual driving styles effectively from the driver's G-G diagram, enabling applicability to large-scale unlabeled data for driving style assessment. The extraction of spatio-temporal characteristics can improve the interpretability of the results obtained using machine learning algorithms. All these results can be used to create a driver's risk profile and provide tailored feedback for improving driving safety.**

***Index Terms*—Driving style assessment, G-G diagram, large-scale driving data, risk profile, unsupervised approach**

I. INTRODUCTION

Driving style, which has been defined in the literature as the way a driver habitually drives a car [1], [2], has a significant impact on road safety and fuel consumption [3]. It has been reported that inappropriate driving behavior is the main reason for accidents [4]. Drivers' aberrant driving behaviors can also lead to an increase in fuel consumption and vehicle emissions [5]. In addition, drivers' different driving styles play an important role in the stability of traffic flow [6], [7]. It has been shown that the formation and propagation of traffic oscillations are related to the variation in drivers' driving styles, particularly in the absence of lane change [7].

Recently, the use of various sensors, such as accelerometers, gyroscopes, and GPS in driving recorders and smartphones have facilitated the collection of large-scale driving data. This has provided a wealth of information on the daily driving behavior of drivers. The data obtained from these sensors, also referred to as naturalistic driving data in the literature [8], recorded the driver's driving behavior, such as the speed and acceleration, in an unobtrusive environment. These data contribute to a more accurate and objective evaluation of driver's driving behavior.

Analyzing a driver's driving style based on these data plays an important role in several applications that are used to improve a driver's driving behavior to reduce traffic accidents and fuel consumption, including driving feedback provision and usage-based insurance (UBI). A driving education program that provides tailored feedback on the on-road performance of drivers can improve road safety and fuel consumption effectively [9], [10]. Additionally, insurance companies are adopting UBI schemes wherein the premium amount is determined based on the driver's driving behavior. In UBI schemes, high-risk drivers are penalized by increasing the premium amount, whereas low-risk drivers are provided incentives by reducing the premium amount. Hence, UBI schemes encourage drivers to adopt a safe and eco-friendly driving style.

A good and accurate assessment of a driver's driving style underpins these applications. There are generally two popular methods to assess a driver's driving style in the literature. One popular method is to classify drivers into several homogeneous groups based on their driving behavior. However, this classification approach may overlook the heterogeneity in the driving styles of the drivers because they generally exhibit

Manuscript received XXXX; revised XXXX. This work was supported by a Grant-in-Aid for Scientific Research from the Takata Foundation in Japan and partially supported by JST COI under Grant number JPMJCE1317" *(Corresponding author: Yuanfang Zhu).*

Yuanfang Zhu is with the Civil and Environmental Engineering Department, Nagoya University, Nagoya 4648603, Japan, (e-mail: zhu.yuanfang.s8@s.mail.nagoya-u.ac.jp).

Meilan Jiang is with the Institute of Innovation for Future Society, Nagoya University, Nagoya 4648603, Japan, (e-mail: jiangml@trans.civil.nagoya-u.ac.j*p*).

Toshiyuki Yamamoto is with the Institute of Materials and Systems for Sustainability, Nagoya University, Nagoya 4648603, Japan, (e-mail: yamamoto@civil.nagoya-u.ac.j*p*).

Naikan Ding is with the Intelligent Transportation Systems Research Center, Wuhan University of Technology, Wuhan 430063, China, (e-mail: nkding@whut.edu.cn).

Hiroko Shinkai is with the Institute of Innovation for Future Society, Nagoya University, Nagoya 4648603, Japan, (e-mail: shinkai.hiroko@mirai.nagoya-u.ac.jp).

Hirofumi Aoki is with the Institute of Innovation for Future Society, Nagoya University, Nagoya 4648603, Japan, (e-mail: hiro.aoki@nagoya-u.jp).

Kan Shimazaki is with the Faculty of Biology-Oriented Science and Technology, Kindai University, Kinokawa 6496493, Japan, (e-mail: shimazakikan@waka.kindai.ac.jp).

diverse styles owing to their different characteristics, such as personality and driving experience. Another popular approach is to score the driver's global driving style (e.g., overall performance of a driver) or specific driving style (e.g., acceleration maneuvers), or both. Each driver can be scored differently, which represents the individual driving risk.

Several parameters, such as speed, acceleration, jerk, speed difference and time gap, have been used for driving style assessment in the literature. Among them, acceleration has been more frequently selected as the metric for driving style assessment [3] because of its representativeness of a driver's driving style. Acceleration can reflect the driver's intentions and preferences directly [11] and was considered as the only parameter that purely described one's driving style [12]. Previous studies have indicated that longitudinal and lateral accelerations are representative of a driver's actions and can be used to distinguish drivers' driving styles [13], [14]. The two axes of accelerations can be considered as a direct reflection of the driver's maneuvers, which are selected based on his or her perceived risk for controlling the vehicle. Moreover, the heterogeneity in drivers' acceleration styles has a significant impact on road safety, fuel consumption [3], [15], and the stability of traffic flow [16]. Additionally, collecting accurate acceleration parameters with conventional data acquisition systems (DAS) appears to be much easier compared to other parameters (i.e., time gap and speed difference). Hence, the modelling method based on acceleration parameters can be widely applied to the driving behavior analysis for ITS. Therefore, the current study focused on modelling a driver's acceleration style using lateral and longitudinal acceleration parameters.

While many studies assumed the longitudinal and lateral accelerations as independent variables, a method that combines both parameters to characterize a driver's driving style in the literature is the G-G diagram. The shape of the G-G diagram for a common driver was observed to be rhomb [13], [17], showing that the magnitude of the longitudinal acceleration likely correlated with that of lateral acceleration. Hence, it is possible that the combination of safe longitudinal and lateral accelerations defined in previous studies is risky for drivers [17]. The G-G diagram has been proven to be an intuitive and effective way to characterize vehicle-driver performances in [13]. Hence, several studies have utilized the G-G diagram to classify drivers' driving styles [18]–[20] and score their individual driving behavior [17]. However, the classification thresholds were determined based on the labeled data obtained from on-road experiments. Regarding large-scale naturalistic driving data, it is time-consuming to label all the collected data. Further, it is open to the subjective assessment of individuals [21]. Additionally, several previous researches encoded the shape of the G-G diagram manually to characterize individual driving/riding styles [13], [17], [22], which are also subject to human judgement.

Machine learning algorithms have been adopted in numerous studies to assess the driving behavior of drivers. Many of them used supervised algorithms to model a driver's driving style [23]–[25], which required a labeled dataset. However, in the context of ITS, large-scale unlabeled driving data have become increasingly prevalent. As mentioned in [21], one of the main challenges in driving behavior analysis for ITS is the increasing prevalence of big data. Unsupervised machine learning algorithm has been considered as a promising approach to process these large-scale data since it does not require a labeled dataset. However, unsupervised algorithms have been relatively less used in assessing the driving styles, particularly in modeling individual driving styles in previous research. Additionally, to the best of our knowledge, none of the previous studies used unsupervised machine learning algorithms to develop a framework for the assessment of a driver's driving style based on the G-G diagram. The utilization of unsupervised approach can address the aforementioned issues in previous research which are related to the G-G diagram. Further, it makes it possible to apply the G-G diagram to large-scale naturalistic driving data to effectively assess a driver's driving style.

Furthermore, the spatio-temporal context of the risky driving behavior of drivers has rarely been considered in previous studies. However, the spatio-temporal distributions of these behaviors can provide implicit factors on a driver's risky driving patterns, such as road topology and intentional behavior. This can facilitate the interpretation of the model. Additionally, providing context information to drivers contributes to safe driving. As such, they can avoid challenging circumstances (e.g., driving at night and risky behavior hotspots) to reduce risky maneuvers.

The purpose of this paper is to develop a framework that combines lateral and longitudinal accelerations to assess a driver's driving style based on large-scale unlabeled driving data. Unsupervised machine learning algorithms are utilized to address the aforementioned issues that hinder the application of G-G diagrams to large-scale driving data. The spatio-temporal context is incorporated into the framework to improve the interpretability of the results obtained by machine learning algorithms and provide useful insights into understanding drivers' risky acceleration behaviors.

The proposed framework includes the definition of safe driving area, two-stage clustering, and extraction of spatio-temporal context. First, a safe driving area is predefined based on the distribution of all drivers' driving data to distinguish risky driving maneuvers from the safe ones. Further, we utilize hierarchical clustering algorithm to classify the driver's average driving behavior into high-, medium-, and low-risk groups. During the second stage, a unique Gaussian mixture model (GMM) is trained for each driver. Each component is labeled with a risky driving pattern category using a statistical method. A driving performance score is calculated based on the probability and severity of the patterns. Further, a driver's numerous risky driving events are decomposed into several risk components. The drivers' self-reported crash data is used to prove the validity of the calculated score. Finally, the spatio-temporal context of the driver's risky driving behavior is extracted. Individual behavioral hotspots are created to show locations with relatively higher frequency of the occurrence of corresponding risky driving pattern. The risk profile for each

driver was created based on the results of the proposed method. A large-scale driving recorder (DR) dataset containing 830,338 km of driving data from 71 drivers was used to perform the proposed method.

The remainder of this paper is structured as follows. Section II presents a detailed literature review. Section III introduces the dataset used in this study. Section IV presents the details of our framework. Section V presents the results and analysis. The contributions and limitations of this study are discussed in Section VI. Finally, conclusions of this study and the potential application of the proposed framework are presented in Section VII.

II. LITERATURE REVIEW

Our research aims to develop a framework to assess a driver's driving style based on G-G diagram using unsupervised machine learning algorithms. The modelling method is based on acceleration parameters and, thus, focuses on a driver's acceleration style. Hence, in this section, we first review studies that model drivers' acceleration styles. Further, we review studies related to G-G diagrams and those wherein an unsupervised approach was used to assess the driver's driving styles.

A. Driver's acceleration style modelling

In previous studies, acceleration parameters have been widely used for driving style assessment because of its representativeness of a driver's driving style and significant impact on road traffic systems. The longitudinal accelerations correspond to acceleration (speeding up) or braking events and its value can be used to evaluate the smoothness of these events. The lateral accelerations correspond to turning events and its magnitude can be used to evaluate the smoothness of the events. Unsmooth acceleration maneuvers are generally associated with aggressive driving behaviors, which increases crash risk and fuel consumption [3].

Reference [26] defined three levels of intensity for acceleration, braking and turning events based on the magnitudes of longitudinal and lateral accelerations. A score was calculated for each driver using the frequency and intensity of the events. In [27], two weighted scores were calculated for measuring a driver's acceleration and braking performances, respectively. The scores were calculated using the frequency of the maneuvers, and the weights were determined based on the magnitudes of the longitudinal accelerations. In [28], acceleration, braking and turning maneuvers were classified into aggressive, normal, and cautious categories based on the statistical features of these maneuvers. A driver's driving performance was evaluated using the proportion of each category of driving maneuvers.

In these studies, the magnitudes of accelerations were used for assessing driving risk partly because a larger acceleration magnitude is more likely to exceed a driver's driving capability, which increases driving risk. Several studies considered both vehicle dynamics and drivers' driving capability (driving behaviors) to model drivers' driving style. Reference [29] proposed a model that considers the vehicles' physical capabilities and drivers' behaviors to assess drivers' acceleration styles. The model was proved to be effective in modelling the aggressiveness of the drivers. Recent studies proposed a physics-informed framework for modelling the aggressiveness of a driver's longitudinal acceleration maneuvers [15], [30], [31]. In the framework, three curves in the acceleration–speed plane were defined to represent a vehicle's acceleration capacities and a driver's ordinary driving behaviors. Based on the three curves, an independent driving style (IDS) metric, that is independent of speed and the vehicle's powertrain, was developed to model the aggressiveness of a driver's acceleration style. The distribution of IDS values can be used to model inter-driver heterogeneity [30], explore the relationship between CO_2 emissions and acceleration style [15], and simulate driver heterogeneity in microscopic traffic simulation [30].

However, most previous studies did not consider the relationship between lateral and longitudinal accelerations or even neglect lateral accelerations to model driving style. Since lateral acceleration plays an important role in road traffic system [3] and there is evidence that the magnitude of longitudinal acceleration is correlated with that of lateral acceleration, it is necessary to combine them for acceleration style assessment. This is typically achieved using a G-G diagram. In the next subsection, we introduce the G-G diagram and review the related studies.

B. Driving style assessment based on G-G diagram

The G-G diagram is a graph that displays lateral and longitudinal accelerations on the x- and y-axes, respectively, which are normalized with respect to gravity. Each point in the diagram represents the driver's instantaneous acceleration maneuver, which is selected based on his or her perceived risk. Fig. 1 shows an example of the G-G diagram of a driver.

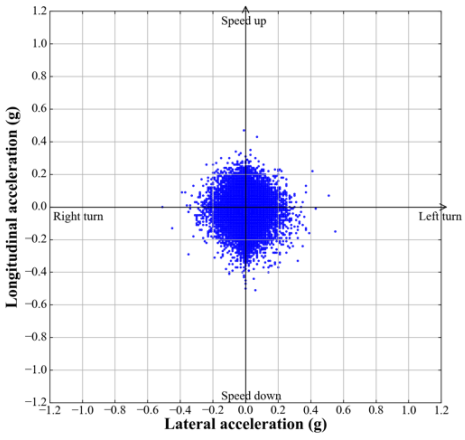

Fig. 1. G-G diagram for a driver

In early studies, the G-G diagram was used for characterizing vehicle–driver performance [13], [32]. An elliptic curve was derived using the maximum-friction restriction of the vehicle to represent its acceleration capacity in the diagram. Furthermore, the shape of the G-G diagram, or the distribution of the data points, was used to characterize driver performance. It has been

shown that only racing drivers are able to fully exploit the vehicle's acceleration capacity and produces an ellipse-shaped G-G diagram. In contrast, common drivers can only exploit a small amount of the vehicle's acceleration capacity and produces a rhomb-shape G-G diagram, which may represent a common driver's actual driving capability [13].

Because the vehicle's capacity and a driver's driving capability can be explicitly depicted in the G-G diagram, recent studies attempted to use it to assess a driver's driving style. In these studies, a safe driving area was defined based on the vehicle's acceleration capacities or driver's driving capability, or both. Data points outside the safe driving area were assumed to be risky maneuvers and the percentage of risky maneuvers was used to assess a driver's aggressiveness or risk level. In [18], drivers were classified into aggressive and non-aggressive groups based on the percentage of risky acceleration maneuvers. In another study, a safe driving area was obtained in a speed-acceleration plane based on the vehicle's acceleration capacity in the G-G diagram [20]. Drivers were classified into high, medium, and low risk groups based on the frequency of risky behaviors. These studies considered the relationship between lateral and longitudinal accelerations for driving style assessment, and the derived safe driving area may be accurate in a specific context. However, there are two issues that hinder the wide application of G-G diagrams for driving style assessment, particularly when using large-scale driving data. First, the safe driving area was derived using the maximum permissible friction and was hence affected by several factors, including the road condition. Therefore, applying it in different contexts (e.g., drivers in different countries) requires the efforts of transportation experts to adjust the parameters of the safe driving area. Second, the classification thresholds in these studies were determined based on labeled data obtained from on-road experiments [2], [18]. During the experiment, drivers were required to drive along a designated route, and the driving performance was labeled "aggressive" or "non-aggressive" based on a subjective judgement (e.g., the self-evaluation of drivers). However, labeling the data in the case of large-scale naturalistic driving data is difficult and subject to human judgement.

Reference [17] addressed the first issue using a statistical method. In this study, a safe driving area was obtained based on the distribution of all drivers' driving data and represents the most common driving maneuvers of a specific group of drivers. Driving maneuvers with a relatively lower probability of occurrence among these drivers are assumed to be risky maneuvers. One advantage of the statistical method is that the safe driving area is determined by the data rather than transportation experts' knowledge. Hence, it can be easily adjusted for use in different contexts. In this study, we also used the statistical method to define a safe driving area in the G-G diagram. More details are presented in Section IV.

In addition, reference [17] used the G-G diagram to score individual driving behaviors. Four levels of risk space (including the safe driving area) were defined in the G-G diagram. A weighted score was calculated for each driver using the percentage of the points in each risk space. Modelling individual driving behaviors can better reflect the heterogeneity in drivers' driving styles compared to] the classification approach. However, this study only used a score to represent a driver's overall driving performance; the performance in terms of specific maneuvers (i.e., braking, turning) was unclear.

In summary, although the G-G diagram is an intuitive and effective way to characterize a a driver's driving style, a framework to apply it to large-scale naturalistic driving data for driver behavior assessment is lacking. To apply it to large-scale driving data, there is need to address several issues in related studies, such as the classification thresholds obtained using labeled datasets and manual encoding of the G-G diagram shape. Unsupervised machine learning algorithms provide opportunities to address such issues. In the next subsection, we review the studies using unsupervised approach to assess a driver's driving style.

C. Driving style assessment using unsupervised approach

Unsupervised machine learning algorithm is a machine learning technique that discovers hidden patterns in unlabeled data. In the context of ITS, large-scale driving data are no longer rare because of the improvement in technology, such as the Internet of Things. These large-scale data are generally unlabeled, thereby making it difficult to extract driving patterns from them [33]. Hence, researchers have started using unsupervised algorithms to process these data for the assessment of a driver's behavior.

In [34], hierarchical clustering and principal component analysis were performed on drivers' speed and acceleration data to classify drivers into five groups, which represents different levels of aggression. Reference [35] proposed a two-stage clustering method to classify the driving styles into six categories based on the harsh event frequency, acceleration, speed, and mobile usage. The k-means algorithm was used for classification at both stages. In these studies, machine learning algorithms were used to classify the average driving behavior of the drivers into several homogenous groups, which may overlook the individual differences in the driving style among drivers in the same group.

A few studies have attempted to use unsupervised algorithms to model individual driving behaviors. Reference [36] utilized self-organization map and k-means algorithms to identify driving patterns in the driving events of all the drivers. The frequencies of potential aggressive driving patterns were displayed in a driving behavior map to establish a diagnosis for each driver. In [33], self-organization maps and k-means algorithms were used to recognize unique driving patterns in drivers' speed and longitudinal and lateral acceleration data. The recognized driving patterns can be labeled with a suitable description found in the literature. In these studies, unsupervised algorithms were applied on the driving data of all drivers. The probability of each driving pattern varied per driver. However, the severity of the pattern (e.g., magnitude of the acceleration) was assumed to be identical for all the drivers. Hence, a risk score considering both the probability and severity of risky driving behaviors was not given.

Of all the unsupervised machine learning algorithms, the

Gaussian Mixture Model (GMM) has been widely used to profile a person, such as speaker and driver recognitions in previous studies [37], [38]. GMM is a probabilistic model that is a weighted sum of Gaussian component densities [37] and is a powerful tool for the statistical modeling of data, such as pattern recognition [39]. Hence, several studies have adopted GMM to model individual driving behaviors. In [38], two GMMs were trained for a standard driver (e.g., the average behavior of all the drivers and safest driver) and target driver, respectively. The similarity between both GMMs was used to score the target driver to measure the driving risk. In [40], the driving data for each driver were fitted with a GMM. The Kullback-Leibler divergence was used to measure the similarity between the distributions of the driving data. An unsupervised clustering algorithm was developed to classify the drivers into three groups based on similarity. In these studies, the uniqueness of the driver's driving behavior was represented by the feature distributions of that driver, which were estimated using GMM. One motivation for using GMM to estimate feature distributions is because the components of the GMM can model some underlying sets of hidden clusters [37] which may correspond to driving patterns. These components reflect some useful driving pattern characteristics for modeling individual driving behaviors. Because of its suitability in modeling individual behaviors, GMM was adopted to encode the distribution (shape) of the G-G diagram to characterize individual driving styles in this study. Particularly, the parameters of each component (e.g., weight and centroid) reflect the category, probability, and severity of the driving pattern, which can be used in scoring the drivers directly. The details are provided in Section IV.

Summarily, few studies have utilized unsupervised machine learning algorithms for driver profiling. Additionally, one of the main limitations of machine leaning algorithm is its interpretability. The spatio-temporal context of a driver's risky driving behavior is one way to improve the interpretability [24], [41]. Furthermore, the spatio-temporal distributions of risky behaviors (e.g., individual behavioral hotspots) can be used as part of the driver's profile for feedback [41]. However, they were hardly considered in previous studies that assessed the driver's behavior using machine learning algorithms.

III. DATA SOURCE

The data used in this study were obtained from the elderly driver database of the Nagoya University Center of Innovation (COI) project. Participants were recruited from among elderly residents in and outside Nagoya City. All the participants were informed about the study and were required to provide informed consent to participate in the experiment according to the requirements of the Nagoya University Ethics Committee (Approval number:2022-16).

A driving recorder (DR) was installed in the drivers' private vehicles to collect daily driving data. The Yupiteru BU-DRHD421 DR was used in all vehicles, and the installation procedure of each DR was identical. Hence, there is no inherent noise in the collected driving data. The DRs collected the timestamp, speed, three axes of the acceleration, and GPS location of the vehicle with a frequency of 1 Hz. The dataset contained the driving data of 85 drivers that are collected from February 2015 to 2019. After checking the driving videos, 14 drivers were not found to be primary drivers during the data collection period. Hence, they were excluded from our dataset, and the driving data of the remaining 71 drivers were used. The total driving distance was 830,338 km. The drivers' ages ranged from 54 to 87 years (mean=72.61, standard deviation = 6.97).

The acceleration data were checked using the G–G diagrams of the drivers. Abnormal values, such as extremely high accelerations, were excluded from the driving data because these values typically exceed the physical maximum values of the vehicle. The timestamp, GPS location, and acceleration data were used as the input of the proposed method. Because the input data are drivers' long-term driving data, we can detect more reliable and stable driving patterns [42], [43], which can provide valuable insights into understanding a driver's driving style and can be used to enhance the benefits of intelligent vehicles (e.g., driving assistance systems) [43].

IV. METHODOLOGY

Fig. 2 illustrates the overall framework of the proposed method. In the framework, two-stage clustering was performed. The first stage classified drivers' average driving behaviors, and the second stage diagnosed individual driving behaviors. Driver classification provides a macroscopic representation of the inter-driver heterogeneity [30], and the semantic label (e.g., high-risk) can facilitate driving feedback provision. The individual driving behavior diagnosis was customized for each driver and provided more details on the heterogeneity in drivers' driving styles. Results of the two approaches are complementary, which provides a more comprehensive understanding of a driver's driving style. More importantly, a normalized performance score was calculated for each driver in the second-stage clustering, wherein the baseline for normalizing the scores was based on the first-stage clustering results (i.e., the average value of the safest group). Because the minimum and maximum values are unusual [27], using them to normalize the scores may lead to biased results. Hence, we adopted a cautious strategy wherein the baseline was determined based on the results of the first-stage clustering.

Before performing the two-stage clustering, a safe driving area in the G-G diagram was defined using a statistical method to detect the risky acceleration maneuvers of the driver. The first-stage clustering is for driver classification. Two variables were developed from the G-G diagram for the first-stage clustering: the percentage of the risky maneuvers and driving instability index. Hierarchical clustering was performed to classify the average driving behavior of drivers into several groups with different risk levels. The number of clusters was determined based on the silhouette index. The second-stage clustering is for individual driving behavior diagnosis. Because the input data is a large-scale dataset, the number of data points is too large to analyze directly. In practice, some data with similar values can be considered as one behavior category because of the fuzziness of driving behaviors [44]. Hence, a unique GMM was trained for each driver to detect risky driving

patterns from numerous risky maneuvers. The driving performance score was calculated based on the probability and severity of the patterns. The scale of the scores was constrained to 0–100 using the average value of the safest drivers obtained in the first-stage clustering. The contribution of each risky driving pattern to the driver's driving risk was calculated. Further, the spatio-temporal context of drivers' risky driving patterns was extracted to improve the interpretability of the results obtained by machine learning algorithms. The temporal distribution of the risky driving patterns of the drivers were calculated, and their behavioral hotspots were created to show intersections with a relatively higher frequency of risky maneuvers. Finally, the risk level, driving performance score, driving risk component, and spatio-temporal characteristics can be used to create the driver's risk profile. In the following subsections, we present the details of the proposed method.

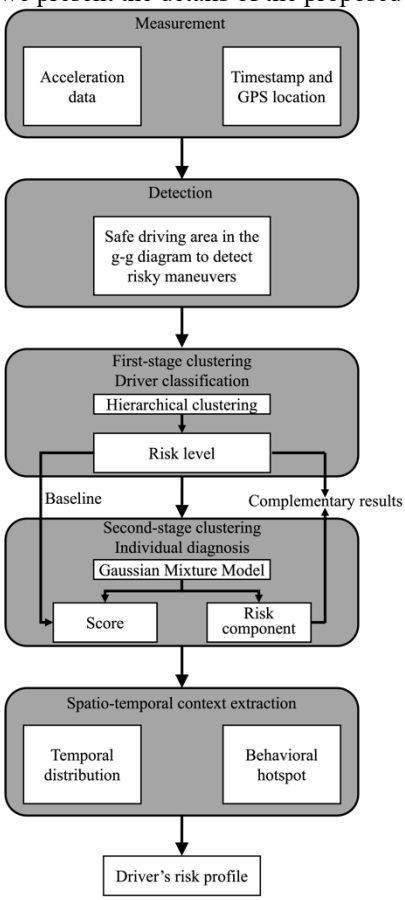

Fig. 2. Overall framework of the proposed method

A. Safe driving area

The safe driving area was obtained using a statistical method to represent the most common acceleration maneuvers of a specific group of drivers. Our assumption is that maneuver with a relatively lower probability of occurrence is risky. This assumption is reasonable because risky driving behaviors are rare, and several previous studies have treated low-probability driving behaviors as risky ones [17], [45], [46].

A confidence region was estimated from the distribution of all the drivers' data points to represent the most frequent behavior. To this end, the distribution of the data points needs to be estimated, and then the confidence region can be calculated.

(1) Estimation of data point distribution

The G-G diagram plane is divided into grid cells of a fixed size. The density of the data points in each grid cell is used to estimate the distribution, and is calculated using the following equation:

$$d_j = \frac{N_j}{\sum_{i=1}^{C} N_i}, \tag{1}$$

where d_j is the density of data points in cell j; N_j represents the number of data points in cell j and C the number of cells in the plane.

(2) Estimation of the confidence region

The distribution of the data points was estimated using the calculated densities of all the cells. The confidence region of the distribution needs to be estimated to represent the most frequent data points (maneuvers). To this end, the densities of all the cells were first sorted in descending order:

$$\boldsymbol{d'} = \{d'_1, d'_2, d'_3, \dots, d'_C\} \, (d'_1 \geq d'_2 \geq d'_3 \geq \cdots \geq d'_C) \tag{2}$$

The cumulative sum of $\boldsymbol{d'}$ can be represented as:

$$\boldsymbol{D} = \{D'_1, D'_2, D'_3, \dots, D'_C\}, \tag{3}$$

where D'_j is the sum of the first j densities in $\boldsymbol{d'}$.

The q confidence region is the cell corresponding to the first k densities in $\boldsymbol{d'}$, and k is calculated using the following equation:

$$k = arg\max_{k}\{D'_k \mid D'_k \leq q\}. \tag{4}$$

The q confidence region of the distribution of all drivers' data points was used as the safe driving area to distinguish risky acceleration maneuvers from the safe ones. The method to determine q is presented in Section V.

B. First-stage clustering

The first-stage clustering classified the average driving behavior of drivers into several homogenous groups, and each group was labeled with a risk level. Two variables were calculated from the driver's G-G diagram for the clustering. The first variable is the percentage of risky acceleration maneuvers, which has been used in several past studies [2], [18]. The second variable is the driving instability index, which is the average distance between all the data points and their centroid. It can be calculated using the following formula:

$$I = \frac{\sum_{i=1}^{n} \sqrt{(x_i - \bar{x})^2 + (y_i - \bar{y})^2}}{n}, \tag{5}$$

where x denotes lateral acceleration, y longitudinal acceleration, (x_i, y_i) data point i in the G-G diagram, and $(\bar{x}, \bar{y})$ the centroid of all the data points. This variable measures the stability of acceleration maneuvers, with a larger value indicating more unstable driving.

The hierarchical clustering algorithm was selected as the first-stage clustering algorithm. It is a widely used unsupervised machine learning algorithm that groups similar objects into clusters. There are two types of hierarchical clustering strategies: agglomerative and divisive approach [47]. The agglomerative approach was used in this study. The agglomerative approach treats each observation as one cluster

at the initial stage, and the dissimilarity matrix of pairwise dissimilarities between two clusters is calculated based on the linkage criterion. In each step, the two most similar clusters are identified and merged into one cluster based on the dissimilarity matrix. By repeating this process, the clusters are merged into more inclusive clusters until all the observations are merged into one cluster [47]. Ward's method [48] was used as the linkage criterion for clustering.

One challenging problem with unsupervised algorithms is finding the optimal number of clusters. In this study, the silhouette index was adopted to determine the number of clusters for first-stage clustering, as used in several previous studies to find the optimal number of the category of driver behavior [35], [49]. The silhouette index measures how close each data point is to its own cluster compared to other clusters [50]. The silhouette index is the average silhouette width of all the data points in one cluster. The silhouette width of data point *i* can be calculated using the following formula:

$$s(i) = \frac{b(i)-a(i)}{max\{a(i),b(i)\}}, \quad (6)$$

where $a(i)$ is the average distance between data point *i* and all the other data points in the same cluster and $b(i)$ the average distance between data point *i* and all the data points in the closest cluster. The silhouette index lies between -1 and 1. A value close to 1 shows that the data points are well-clustered and assigned to an appropriate cluster, whereas a value close to -1 shows that the data points are likely to be misclassified.

C. Second-stage clustering

Second-stage clustering identifies risky driving patterns from risky acceleration maneuvers for each driver. The second-stage clustering process is shown in Fig. 3. Numerous risky events of the driver were clustered into several similar groups. A statistical method was used to label each cluster based on its centroid.

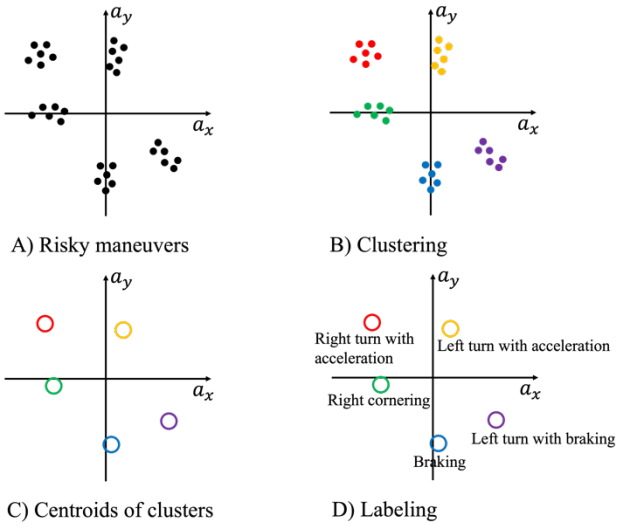

Fig. 3. Second-stage clustering process

GMM was adopted for the second-stage clustering because of its suitability in modeling individual behavior. A GMM is a weighted sum of a finite number of Gaussian distributions, as expressed by the equation below [37]:

$$p(\boldsymbol{x}|\lambda) = \sum_{i=1}^{K} \alpha_i \, p(\boldsymbol{x}|\boldsymbol{\mu_i}, \Sigma_i), \quad (7)$$

where $\boldsymbol{x}$ is a 2-dimensional feature vector in this study, and $p(\boldsymbol{x}|\boldsymbol{\mu_i}, \Sigma_i), i = 1, \ldots, and\ K$ is the probability density function of the *i*th component. Each component is a 2-dimensional Gaussian distribution with mean vector $\boldsymbol{\mu_i}$ and covariance matrix Σ_i. α_i is the weight of the *i*th component and is subject to the constraint $\sum_{i=1}^{K} \alpha_i = 1$.

A unique GMM model was fitted with each driver's risky acceleration maneuvers. The expectation-maximization (EM) algorithm was used for parameter estimation. The number of components was determined based on the Bayes information criterion (BIC) score, which is a well-performed indicator for selecting the number of components [51]. It can be calculated as

$$BIC = -2log\left(L(\psi)\right) + klog(N), \quad (8)$$

where $L(\psi)$ is the observed likelihood of the mode, k the number of parameters in the model, and N the number of training data points. A lower BIC score indicates a better performance of the estimated model. In this study, the number of components was selected so that the BIC score of the model did not substantially decrease with an increase in the number of components.

In the estimation result, each component is a cluster, and the mean vector of the component Gaussian density $\boldsymbol{\mu_i}$ represents the centroid of the cluster. The weight of each component α_i represents the percentage of data points that have been clustered into this group. Hence, it can be interpreted as the probability of one random risky maneuver belonging to this cluster.

The centroids of the components are used to label the components. Reference [52] divided the G-G diagram into nine areas, and each area was labeled with a specific category of acceleration maneuvers. However, their study was for racing drivers. Since a common driver's driving behavior is different from that of a racing driver [13], the thresholds for the division of the G-G diagram in their study cannot be used directly in our study. Following their nomenclature, a statistical method was used to label the component with a suitable semantic description. Based on the observation of the centroids of the components for all drivers, two thresholds were determined according to the 10th percentile of the lateral and longitudinal acceleration magnitudes to define eight risky driving pattern categories. Each component is labeled with one of the following eight risky driving patterns: acceleration, braking, left cornering, right cornering, left turn with acceleration, left turn with braking, right turn with acceleration, and right turn with braking. The detailed results are presented in Section V.

D. Driving performance score and risk component

In past research, a driving performance score is a normalized score to measure a driver's driving risk, and it is calculated based on the frequency and severity of the risky driving behavior [3]. In our study, the estimated GMM for each driver was used to calculate the normalized driving performance score for the driver. TABLE I shows the estimation results of the GMM for one driver. The weight of the component α_i corresponds to the probability of one risky maneuver being part of this component. It is noteworthy that the probability here is

in relation to the driver's risky acceleration maneuvers rather than all the acceleration maneuvers. Hence, it should be multiplied by the percentage of risky acceleration maneuvers to represent the probability of occurrence. The modulus of the centroid of the component was computed to represent the severity of the behaviors. Thus, a risk index for driver *m* can be defined as

$$R_m = P_m \sum_{i=1}^{K} \alpha_i |\boldsymbol{\mu_i}|, \quad (9)$$

where P_m is the percentage of risky acceleration maneuvers for driver *m* and $|\boldsymbol{\mu_i}|$ the modulus of the centroid of the component ($\boldsymbol{\mu_i} = (\bar{a}_x, \bar{a}_y)$), which can be calculated as $|\boldsymbol{\mu_i}| = \sqrt{\bar{a}_x{}^2 + \bar{a}_y{}^2}$. A normalized driving performance score on a scale of 0–100 for driver *m* can be calculated as

$$S_m = 100 \times \frac{R_{baseline}}{R_m}, \quad (10)$$

where $R_{baseline}$ is the average risk index of drivers in the safest group obtained in the first-stage clustering. This value was used as the baseline because the minimum risk index was unusual among drivers. However, this led to scores that are higher than 100. Scores higher than 100 were changed to 100 to ensure that all the scores were in the range of 0–100. Hence, a score of 100 indicates a safer driving style than the average level of the safest group rather than being free of risk.

TABLE I.
ESTIMATION RESULTS OF GMM FOR DRIVER NO. 44

Component	Weight α_i	Centroid $\boldsymbol{\mu_i}$	Label
1	13.25%	(0.05g, 0.26g)	Risky acceleration
2	12.38%	(0.03g, 0.31g)	Risky acceleration
3	7.11%	(0.02g, 0.36g)	Risky acceleration
4	13.83%	(0.11g, 0.21g)	Risky left turn with acceleration
5	12.36%	(0.16g, 0.24g)	Risky left turn with acceleration
6	3.86%	(0.28g, 0.15g)	Risky left turn with acceleration
7	15.49%	(-0.06g, 0.28g)	Risky right turn with acceleration
8	10.56%	(-0.13g, 0.24g)	Risky right turn with acceleration
9	9.44%	(-0.17g, 0.28g)	Risky right turn with acceleration
10	1.73%	(-0.3g, 0.21g)	Risky right turn with acceleration

The driver risk component can be calculated based on the label of the component. Each component was labeled with a risky driving pattern category. It is possible that several components are labeled with the same category, but the probability and severity of the behaviors are different. For risky driving pattern *n*, its contribution to the risk index of driver *m* is calculated using the following formula:

$$C_{m,n} = \frac{P_m \sum_{i=G}^{L} \alpha_i |\boldsymbol{\mu_i}|}{R_m}, \quad (11)$$

where α_i $(i = G, G+1, \ldots, L)$ are the weights of the components corresponding to the risky driving pattern *n* (e.g., 7th–10th components in Table I correspond to the driving pattern of risky right turn with acceleration) and $\boldsymbol{\mu_i}$ the centroids of the corresponding components. The contribution of each risky driving pattern to the risk index is used to calculate the driver's driving risk component.

E. Spatio-temporal context extraction

Spatio-temporal characteristics can provide implicit factors of a driver's risky driving behavior. Additionally, the incorporation of context information can result in a fairer comparison between drivers' driving performances. In [53], the locations of risky driving events for aggressive driving are uniformly distributed, which implies an intentional behavior behind the wheel. Contrarily, the event locations for safe driving are clustered in several specific areas, thereby implicating unintentional behavior due to the road topology. Behavioral hotspots have been used in several studies to display locations with a relatively higher frequency of risky driving behavior [41], [54]. The hotspots in these studies were created based on all the driving events of the drivers and were population behavioral hotspots. While population behavioral hotspots can be used to diagnose problems on intersection or road geometry, this study focused on individual behavioral hotspots and included them in the driver's risk profile for driving feedback provision. For example, a warning message can be sent to a driver before entering high-risk locations. Additionally, the temporal distribution of risky driving behaviors can provide implicit factors related to the traffic volume and road conditions. It can also be provided to the driver as driving feedback.

In this study, the temporal distributions of the identified risky driving patterns for each driver were calculated. Individual behavioral hotspots were created to show intersections with relatively higher frequencies of risky maneuvers. We focused on intersection-level hotspots because drivers in our study live in urban areas where intersections are dense. Furthermore, risky acceleration maneuvers occur more frequently at intersections compared to road segments [55]. First, the locations of the risky acceleration maneuvers were divided into segment locations and intersection locations. In our study, the intersection influence area is circular with 35 m radius. We selected 35 m as the threshold because this value has been widely used to determine whether one traffic collision occurs within an intersection in Japan. The intersection locations were matched with the corresponding intersections. The frequency of risky acceleration maneuvers for each intersection was calculated as the number of locations matched to the intersection divided by the total number of intersection locations. The most frequent

intersections that accounted for 50% of the risky driving pattern occurrences were extracted as hotspots of the pattern and displayed in the map with circle markers. The radius of the circular marker was proportional to the frequency of occurrence at the intersection.

V. RESULTS AND DISCUSSION

A. Safe driving area

In our study, the 95% confidence region of the distribution of all drivers' acceleration data points was used as the safe driving area. This value was selected based on the two-sigma rule and corresponds to $\mu \pm 2\sigma$. Furthermore, the shape of the 95% confidence region is similar to the safe driving area defined in [18] and close to a rhomb shape (Fig. 4). Hence, in this study, the 95% confidence region was selected as the safe driving area to distinguish risky acceleration maneuvers from the safe ones.

Numerous previous studies have not considered the relationship between lateral and longitudinal accelerations when detecting risky acceleration maneuvers. In these studies, two thresholds were set for the lateral and longitudinal accelerations to detect risky lateral and longitudinal maneuvers separately. This corresponds to the rectangular area in the G-G diagram. The orange line in Fig. 4 represents the thresholds used in [26]. As shown in Fig. 4, the rectangular area cannot identify some risky maneuvers that combine the two axes of acceleration. Indeed, all previous studies related to G-G diagrams revealed that common drivers produced rhomb-shaped G-G diagrams rather than rectangular-shaped ones. This shows that the magnitude of longitudinal acceleration is likely to correlate with that of lateral acceleration. Hence, it is necessary to consider the relationship between lateral and longitudinal accelerations to detect risky acceleration maneuvers. The G-G diagram provides an intuitive way to combine both axes of acceleration to characterize the driving style. However, as mentioned in the previous sections, several issues must be addressed when applying it to large-scale driving data. Unsupervised machine learning algorithms were used to address these.

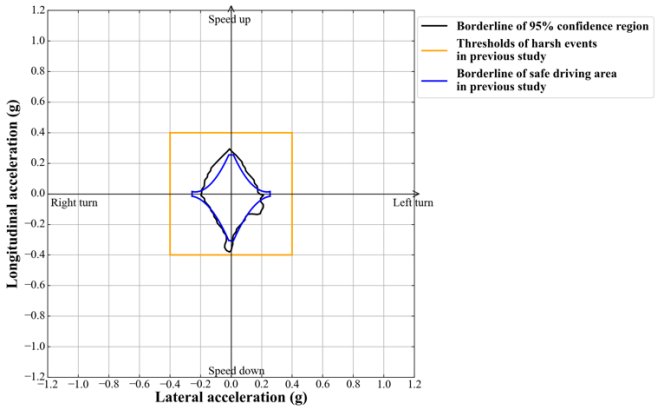

Fig. 4. Thresholds used to detect risky acceleration maneuvers in our study and previous studies: the orange line represents thresholds used in [26] and blue line thresholds used in [18]

B. First-stage clustering

In the first-stage clustering, the number of clusters was determined as three according to the silhouette index (Fig. 5). Fig. 6 shows the clustering results. Each group represents a different risk level of the driver's acceleration maneuvers. Five drivers were classified into the high-risk group. High-risk drivers performed risky acceleration maneuvers more frequently than those in other groups. The average percentage of risky acceleration maneuvers is 17.15%, as displayed in TABLE II. The driving behavior of drivers in the high-risk group are more unstable, and the average driving instability index is approximately 1.42 and 1.93 times that of the medium-risk and low-risk groups, respectively. Compared to high-risk drivers, the risky maneuver frequency of medium-risk drivers was lower, and the average percentage of risky maneuvers was 6.67%. The driving style of low-risk drivers was the safest among the three groups. The risky driving maneuvers of low-risk drivers are unusual, and their driving behavior is stable.

Previous studies have only used the percentage of risky maneuvers to classify the driving style of drivers. In [18], if the percentage is larger than 9%, the driver is categorized as aggressive. In [2], 8% was selected as the threshold to distinguish high-risk drivers from medium-risk drivers. The average percentage of risky maneuvers for high-risk drivers in our study was higher than that in both studies. However, the thresholds in both studies were determined based on the labeled data obtained from on-road experiments. Risky drivers may behave differently in a naturalistic driving environment compared to on-road experiments, which is a possible reason for the higher average percentage in our study. Furthermore, in our study, drivers were classified into three groups without a predefined threshold of the aforementioned variable.

In our study, the driving instability index (a new variable), was developed for the classification. The clustering results prove the reliability of this variable for measuring a driver's driving risk. As shown in Fig. 6, the driving behaviors of drivers in the high- and medium-risk groups are more unstable than those of low-risk drivers. The driving instability index highly correlates with the percentage of risky maneuvers ($r = 0.79, p < 0.001$). Hence, it can be used to replace the percentage of risky maneuvers if only one variable is used for the classification. Furthermore, the driving instability index was calculated using all the data points in the G-G diagram. Thus, it does not require a predefined safe driving area. This shows that it is possible to classify driving styles without any threshold if we use only this variable. For example, if the driving instability index of a new driver is larger than the average level of the high-risk group, the driver can be categorized as a high-risk driver without a need to define a safe driving area.

The first-stage clustering classified drivers into different risk groups based on acceleration parameter alone. The classification results may be biased if other parameters are considered. For example, if a low-risk driver's smooth acceleration maneuvers are performed at high speeds frequently, this driver may be a false "low-risk" driver. Hence, it is necessary to examine whether the classification results can reflect the driving risk of other parameters. Speed was selected

because it is also an important parameter for driving style assessment. Fig. 7 shows the cumulative distribution of the vehicle speed for drivers in different risk groups. Since the speed limit of most urban roads in Japan is 60 km/h or lower, a speed higher than 60 km/h can be considered as a high speed. Interestingly, the frequency of high speed increased with risk level although speed was not an input parameter of the model. This implies that the classification results can not only represent the risk level of a driver's acceleration maneuvers but also reflect the risk level of other driving behaviors, such as speed.

TABLE II.
MEAN VALUE PERCENTAGES OF RISKY ACCELERATION MANEUVERS AND DRIVING INSTABILITY INDEX IN EACH GROUP

Group	Number of drivers	Percentage of external points	Driving instability index
High-risk	5	17.15%	0.131
Medium-risk	13	6.67%	0.092
Low-risk	53	3.12%	0.068

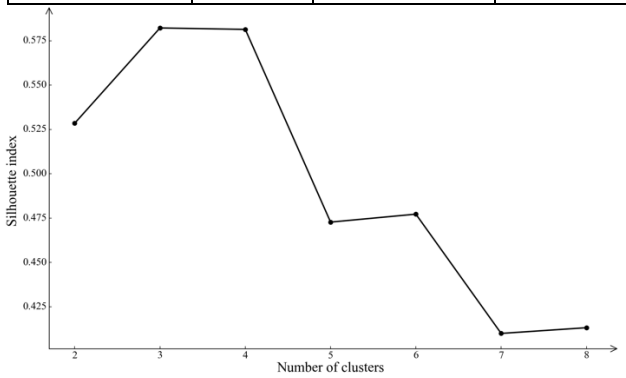

Fig. 5. Silhouette indices for different numbers of the cluster

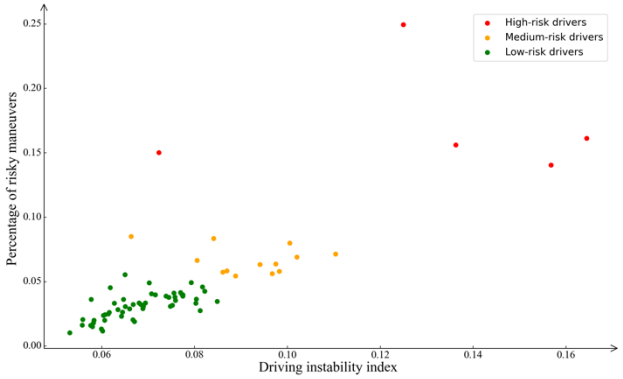

Fig. 6. First-stage clustering results

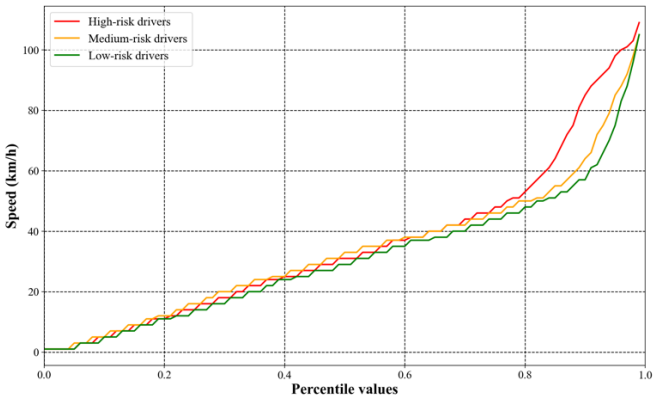

Fig. 7. Cumulative distribution of vehicle speed for drivers in different risk groups

C. Second-stage clustering

In the second-stage clustering, a unique GMM was fitted with each driver's risky acceleration maneuvers. Fig. 8 shows the G-G diagram for driver No. 44. It can be observed from the G-G diagram that this driver's risky driving pattern is related to acceleration (speeding up), and some of these risky maneuvers are a combination of lateral and longitudinal accelerations. However, these characteristics were discovered by manually observing the shape of the G-G diagram. Hence, GMM was utilized to model this driver's risky driving behavior. The number of components was determined based on the BIC score. Fig. 9 shows the BIC scores for different component numbers. After the number of components reached 10, the BIC score did not decrease considerably with an increase in the number of components. This shows that the performance of the model did not improve significantly even if we continued increasing the number of components. Hence, 10 was selected as the optimal number of components. Note that this number was determined automatically by identifying the knee point using our algorithm.

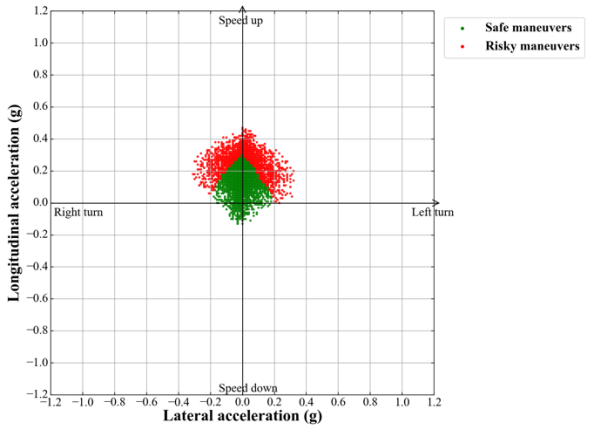

Fig. 8. G-G diagram for driver No. 44

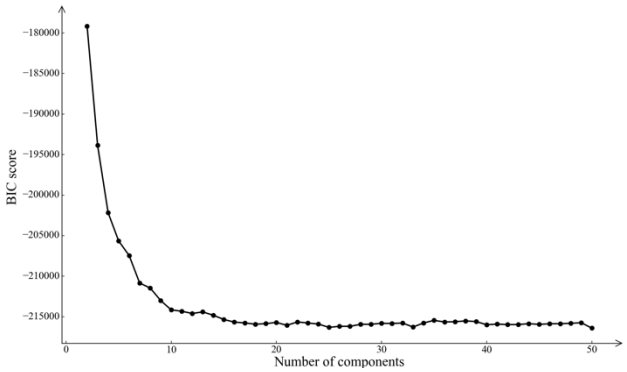

Fig. 9. BIC scores for different component numbers

The estimation results are displayed in TABLE I. The driver's numerous risky maneuvers are clustered into 10 components of the GMM. Each component needs to be labeled with a semantic description to represent the risky driving pattern category. To this end, the magnitudes of the lateral and longitudinal accelerations of the centroids for all the drivers are plotted in Fig. 10. Overall, the magnitude of the longitudinal acceleration decreases with an increase in the magnitude of the lateral acceleration ($r = -0.67, p < 0.001$). Hence, even if drivers drive in a risky manner, the combination of large lateral and longitudinal accelerations is rare. Based on the characteristics observed in Fig. 10, the 10th percentiles of the lateral and longitudinal acceleration magnitudes were first calculated and the values are 0.057 and 0.037 g, respectively. We used slightly smaller values (0.05 and 0.03 g) as the thresholds to distinguish between different pattern categories. Following the nomenclature in [52], eight risky driving patterns were defined, as shown in TABLE III. If the magnitude of the lateral acceleration is smaller than 0.05 g, the magnitude of the longitudinal acceleration is generally much larger than that of the lateral acceleration. Hence, the component is labeled as risky acceleration (speeding up) or braking in this case. Conversely, if the magnitude of longitudinal acceleration is smaller than 0.03 g, the magnitude of lateral acceleration is generally much larger than that of the longitudinal acceleration, and the component is labeled as risky right cornering or left cornering. Otherwise, the component is labeled with the other four categories according to the signs of the two axes of acceleration.

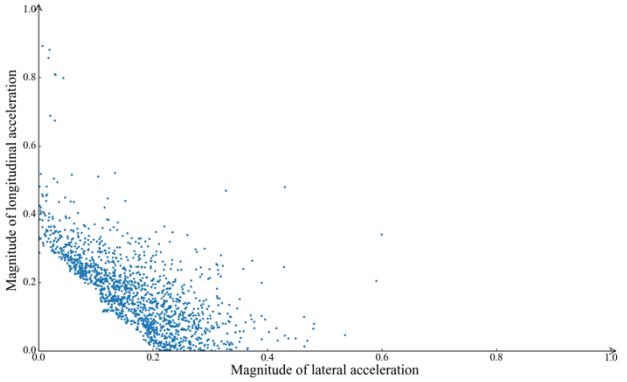

Fig. 10. Magnitudes of lateral and longitudinal accelerations of the centroids for all drivers (1511 centroids altogether)

TABEL III.
DEFINITION OF EIGHT RISKY DRIVING PATTERNS (WHERE a_x AND a_y DENOTE THE LATERAL AND LONGITUDINAL ACCELERATION OF THE CENTROID, RESPECTIVELY)

Definition	Risky driving pattern category
$\|a_x\| < 0.05g$ and $a_y > 0$	Risky acceleration
$\|a_x\| < 0.05g$ and $a_y < 0$	Risky braking
$\|a_y\| < 0.03g$ and $a_x > 0$	Risky left cornering
$\|a_y\| < 0.03g$ and $a_x < 0$	Risky right cornering
$\|a_x\| > 0.05g$, $\|a_y\| > 0.03g$, $a_x > 0$, and $a_y > 0$	Risky left turn with acceleration
$\|a_x\| > 0.05g$, $\|a_y\| > 0.03g$, $a_x > 0$, and $a_y < 0$	Risky left turn with braking
$\|a_x\| > 0.05g$, $\|a_y\| > 0.03g$, $a_x < 0$, and $a_y > 0$	Risky right turn with acceleration
$\|a_x\| > 0.05g$, $\|a_y\| > 0.03g$, $a_x < 0$, and $a_y < 0$	Risky right turn with braking

Based on the definition in TABLE III, each component is labeled with a risky driving pattern category. The labeling results of the GMM for driver No.44 are displayed in TABLE I. It can be found that it is possible that several components are labeled with the same category, but the probability (weight of the component) and severity (modulus of the centroid) are different. Hence, the probability and severity were used to calculate the driving performance score and driving risk component for each driver. Using (10) and (11), the driving performance score and driving risk component for driver No. 44 were calculated, and the results are shown in Fig. 11. Driver No. 44 has been classified into the high-risk group in the first-stage clustering, and the performance score is low: 18/100. Three risky driving patterns have been identified by GMM: risky acceleration, risky right turn with acceleration, and risky left turn with acceleration, which correspond with what is observed from the G-G diagram. However, the density of data points (probability of occurrence) is difficult to observe in the G-G diagram. Conversely, the GMM can model the probability of the behaviors. Furthermore, behaviors corresponding to the same risky driving pattern category (defined in Table III) were divided into different levels of severity. The two variables form the basis for driver profiling [3], [27]. Hence, based on the probability and severity of patterns, driving performance score and risk component were calculated for diagnosing individual driving behaviors. The driving performance score represents the overall performance of a driver's acceleration maneuvers, and the risk component reflects the contribution of each risky

driving pattern category to driving risk. With the proposed method, the shape of the G-G diagram was encoded effectively, and the driver's numerous risky driving events were decomposed into several risk components, which facilitated the driver risk analysis and feedback provision.

Fig. 12 shows the driving risk components of different drivers. We randomly selected 18 low-risk drivers and plotted their risk components as representative examples. Although these drivers' driving exposure and driving context are different, the results are comparable because the drivers' long-term driving data were used to achieve reliable and stable pattern detection results [42], [43]. In addition, all drivers primarily drove their cars in the Nagoya metropolitan area; therefore, the overall traffic conditions can be considered relatively similar. From Fig. 12, we noticed heterogeneity in the risky driving behavior of the drivers. Risky acceleration or risky braking patterns have been identified for all high-risk drivers, and account for a great part of the driving risk for most high-risk drivers. Conversely, both patterns could not be recognized for many low-risk drivers. This shows that risky acceleration and braking of these drivers are very rare and, thus, were not identified as risky patterns by the GMM. Additionally, even though one of both patterns was identified for several low-risk drivers, it accounts for only a smart part of the driving risk in most situations. Further, the combination of lateral and longitudinal accelerations accounts for the majority of the driving risk for low-risk drivers.

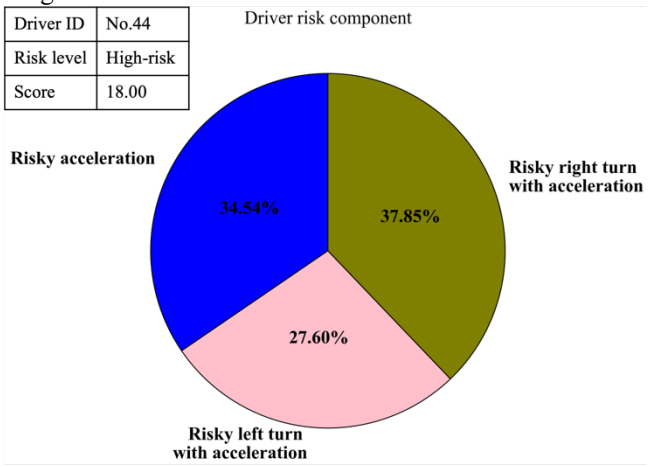

Fig. 11. Risk level, performance score, and risk component of driver No. 44

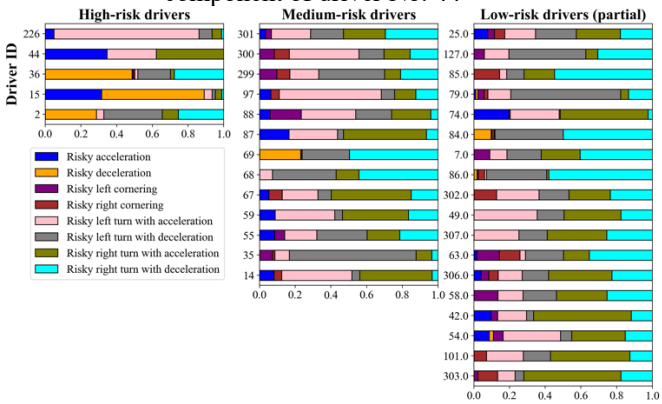

Fig. 12. Risk components of different drivers

D. Validity of driving performance score

In this study, the self-reported crash data of the drivers were used to validate the calculated performance scores. During the DR data collection period, drivers reported their traffic crash experiences annually. Among the 71 drivers, 19 reported that they had been involved in at least one traffic crash, including a minor crash, whereas the remaining 52 reported that they had never experienced a traffic crash. Hence, the drivers were divided into two groups based on self-reported traffic crash data: crash-involved and crash-free drivers. Normality tests revealed that the driving performance score was not normally distributed ($p < 0.01$). Hence, the Kruskal-Wallis (KW) test, a non-parametric method, was performed to verify whether there was a significant difference between the medians of the performance scores in both groups. The results showed that a significant difference existed ($p = 0.001$). Fig. 13 displays the driving performance scores of both groups. Crash-involved drivers were associated with lower driving performance scores (median = 59.39) than crash-free drivers (median = 82.77). Hence, the calculated driving performance score is reliable for measuring the driver's driving risk and might be used to measure the driver's risk of involvement in a crash.

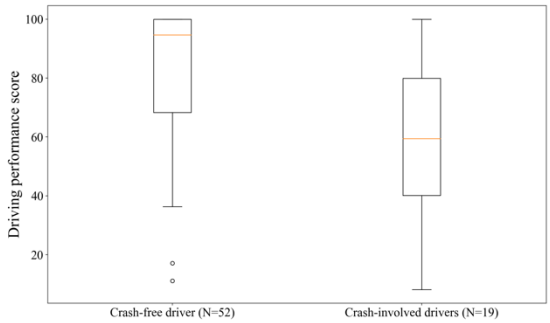

Fig. 13. Driving performance scores in crash-free and crash-involved groups

E. Spatio-temporal context

We selected two drivers from the sample to analyze the spatio-temporal characteristics of their risky driving behaviors. One driver was a high-risk driver with the lowest driving performance score (8.12/100). The other driver was a low-risk driver with a higher score (86.14/100). The two drivers exhibited distinct spatio-temporal characteristics that may imply two risky behavior factors: intentional behaviors and unintentional behaviors caused by the external environment. The temporal distribution of the high-risk driver's risky driving patterns is displayed in Fig. 14. Compared to other risky patterns, risky braking is more likely to occur between 7:00 and 10:00, which corresponds to the morning peak hours in Japan. More than half (58.35%) of the risky braking behavior occurred during this period. A large proportion (39.89%) of the risky acceleration also occurred during the morning peak hours. Compared to risky acceleration and braking, the combination of lateral and longitudinal accelerations is more likely to occur at intersections and between 13:00 and 16:00. Fig. 14 also shows that risky maneuvers occurred much more frequently at

intersections. Hence, an individual behavioral hotspot was created at the intersection level (Fig. 15). First, risky acceleration and braking locations are more uniformly scattered compared to other patterns. The two risky patterns account for the majority of the drivers' driving risk. Numerous risky braking locations are distributed along the artery. In the morning peak hours, the traffic volume of the artery is likely to be high. Thus, frequent risky braking behaviors may imply a close following distance. Additionally, the uniform distribution of the locations show that the risky acceleration and braking behavior of the drivers are likely to be intentional [53]. This is referred to as aggressive driving or bad driving habits in the literature. Contrarily, the locations corresponding to the combination of lateral and longitudinal accelerations are clustered into relatively fewer intersections. This implies that these behaviors are likely caused by the external environment (e.g., road topology).

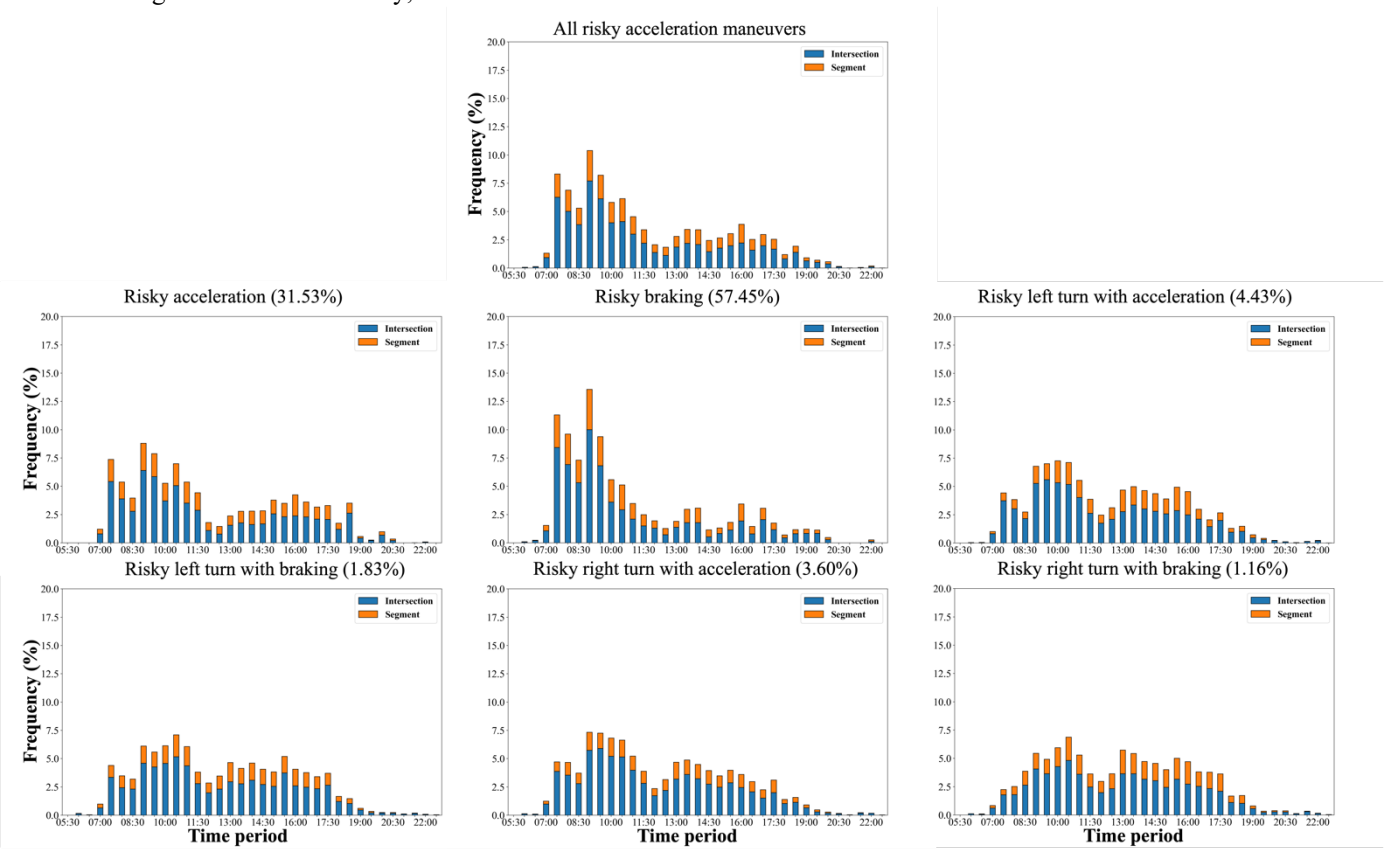

Fig. 14. Temporal distribution of different risky patterns for driver No. 15 (the frequency is the percentage within the corresponding risky patterns)

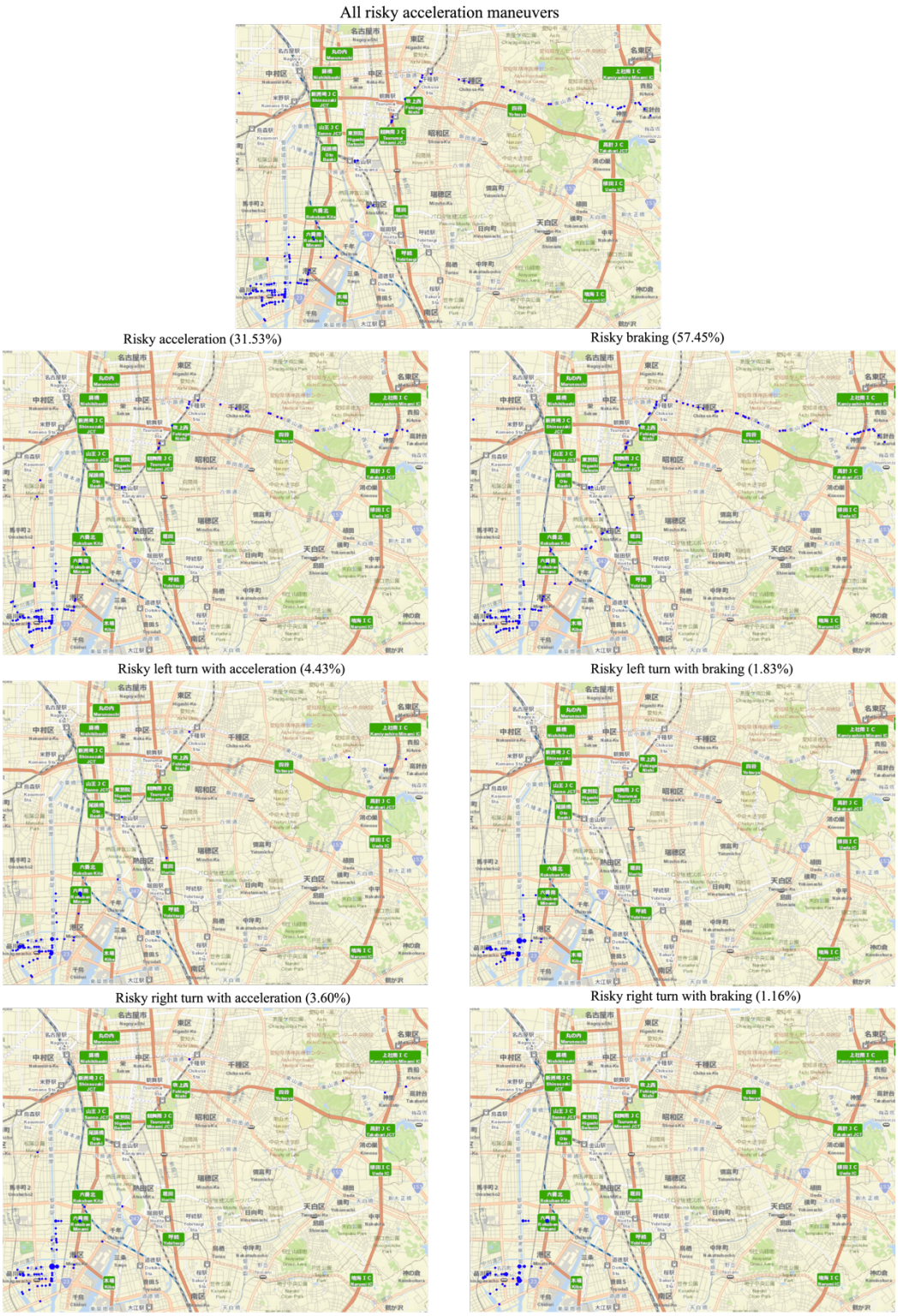

Fig. 15. Intersection-level behavioral hotspot for driver No. 15 (the radius of the circle marker is proportional to the frequency of occurrence)

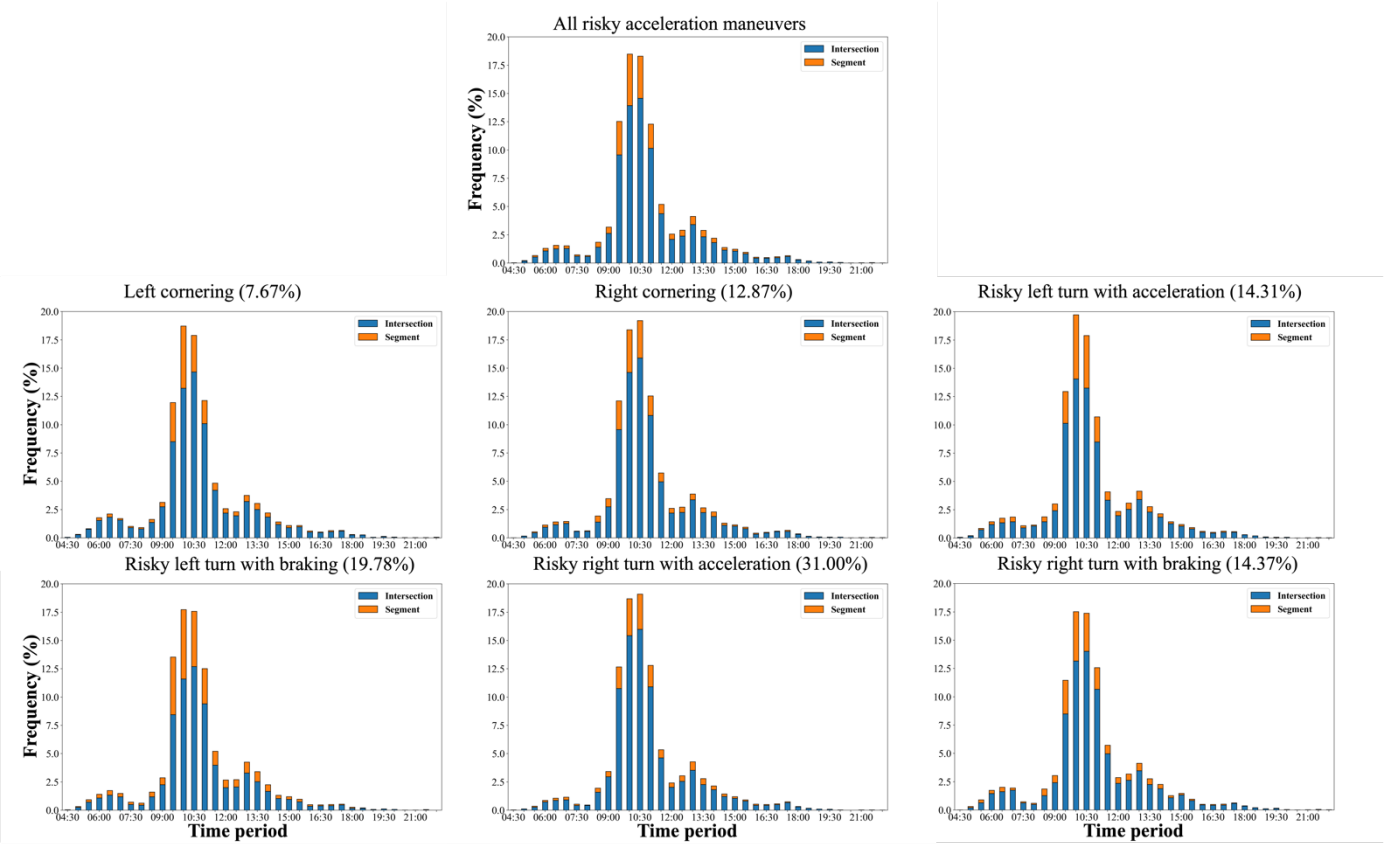

Fig. 16. Temporal distribution of different risky patterns for driver No. 56

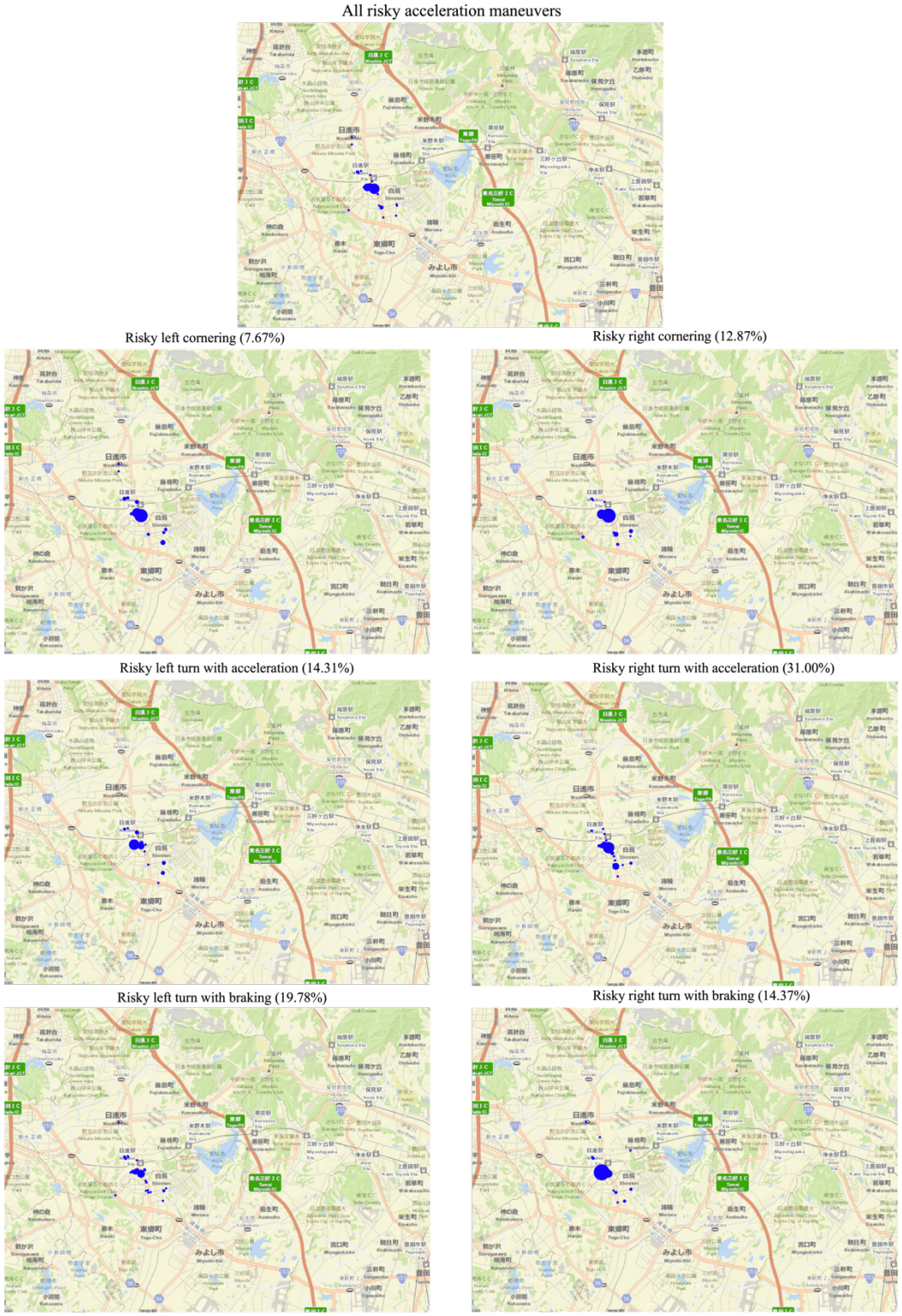

Fig. 17. Intersection-level behavioral hotspot for driver No. 56 (the map scale is the same as Fig. 14)

Fig.s 16 and 17 display the temporal and spatial distributions of driver No.56's risky driving behaviors, respectively. As shown in Fig. 16, the temporal distributions of different patterns are similar. Risky maneuvers are more likely to occur between 9:30 and 11:30. Fig. 17 indicates that a much smaller number of intersections could account for 50% of the occurrence of risky maneuvers compared to that of Driver No. 15. Particularly, the radii of several hotspots are much larger than those of the other intersections. This shows that the risky maneuvers of this driver were likely unintentional and caused by the external environment (e.g., intersection design issues). Hence, it can be inferred that this driver was frequently exposed to these hotspots between 9:30 and 11:30, and that these risky behaviors were likely caused by the external environment, such

as road topology.

The individual behavioral hotspot characterizes the spatial distribution of every driver and, thus, is a microscopic approach. Conversely, a macroscopic approach considers the overall spatial distribution of multiple drivers (e.g., a representative sample of the driving population in a road network). While the former can reflect personalized spatial risk patterns, the latter can better reflect the overall safety performance of a road network and, thus, is more suitable for diagnosing problems on intersection and road geometry. However, our sample contains 71 drivers scattered across the Nagoya metropolitan area, and this number of drivers is not sufficient for such an analysis.

VI. CONTRIBUTIONS AND LIMITATIONS

A. Contributions

The contributions of this study are threefold. First, this study proposed a framework that combines lateral and longitudinal accelerations for profiling drivers. The relationship between both axes of accelerations was considered to assess driving style. This provides more accurate modelling results. Moreover, because the acceleration parameters can be collected by ubiquitous and inexpensive DASs (e.g., smartphones and in-vehicle devices), the proposed framework can be widely applied to driving behavior analysis for ITS. Second, the proposed framework utilized an unsupervised approach for modelling individual driving behaviors. This enables the proposed framework to be applicable to large-scale driving data that becomes increasingly prevalent in the context of ITS. The large-scale driving data are generally collected during a long period. Thus, these data can provide reliable underlying driving patterns. Furthermore, GMM was employed to evaluate a driver's overall driving performance and decompose numerous risky maneuvers into several risk components, which facilitate driving behavior analysis. Third, the spatio-temporal context of risky driving patterns was extracted to improve the interpretability of the results obtained by machine learning algorithms. This can also be included in a driver's risk profile and used for driver feedback provision.

B. Limitations and future work

A) Other driving parameters

One of the main limitations of this study is that the effect of speed was not considered in the framework. Previous studies indicate that there is a non-linear relationship between speed and longitudinal acceleration [29], [30]. However, the relationships among speed, lateral acceleration and longitudinal acceleration are not well-established in the literature. To the best of our knowledge, only two previous studies combined the three parameters for driving performance assessment. However, there is inconsistency in the relationships among the three parameters. Using real-world driving data, reference [13] observed a nonmonotonic relationship between the size of the G-G diagram produced by drivers and speed. The size of the rhomb-shape G-G diagram enlarges from low to medium speeds and, then, shrinks from medium to high speeds. Another study [20] only considered vehicle dynamics to derive a circular safe driving area in the G-G diagram, and the size of it decreased with an increase in speed. Because drivers can only exploit a small part of the vehicle's acceleration capacity, neglecting driving capability may lead to inaccurate results.

Although the effect of speed was not considered, our analysis indicates that the driving risk evaluated by the acceleration parameter alone can also reflect the overall risk of drivers' speed behaviors. Hence, the impact of not considering speed as an input parameter on evaluating driver risk can be considered small. However, drivers' driving risk components will contain more risky driving pattern categories if speed is considered as an input parameter. Hence, for future work, we can investigate the relationships among speed, lateral acceleration, and longitudinal acceleration theoretically by considering the vehicle's capacity and driver's driving capability. Then, the speed can be included in our model to derive a safe driving space and increase the number of risky driving pattern categories.

Furthermore, the data from the front vehicle (e.g., time gap and speed difference) are not available in our dataset. A previous study indicates that there is a strong correlation between large acceleration and short time headway [57]; therefore, the driving risk evaluated in the present study may also reflect the risk level of these behaviors. For future work, we intend to collect and verify these data.

B) Vehicle trajectory reconstruction

In our study, all drivers' driving data were collected using the same system. Hence, there is no inherent noise in the data. However, considering that the proposed framework can be widely applied for driving style assessment, it is expected to be performed using driving data collected with different systems (e.g., different smartphones). In this case, vehicle trajectory reconstruction is necessary to reduce the noise in the data and enable comparability of the results. For example, in [31] a physics-informed adaptive framework is proposed that significantly reduces measurement errors and is widely applicable to different DASs. The incorporation of vehicle trajectory reconstruction can enable applicability of the proposed framework to a wide range of scenarios.

C) Spatio-temporal context

In the present study, we characterized individual spatial and temporal risk patterns separately. However, the spatio-temporal joint effect can provide more useful insights into understanding drivers' risky driving. For future work, a model can be developed to analyze the spatio-temporal joint effect. To this end, we will use a map-matching algorithm to project each GPS location on the road segment to create segment-level hotspots and incorporate temporal context into the behavioral hotspots. Furthermore, a statistical model can be used to analyze the joint effect of spatio-temporal context on a driver's risky driving.

VII. CONCLUSIONS

This paper proposed a framework that combined lateral and longitudinal accelerations to assess a driver's driving style. Unsupervised machine learning algorithms were utilized to classify the average driving behavior of drivers and encode the shape of the G-G diagram to characterize individual driving

behaviors. A driving performance score was calculated for each driver based on the probability and severity of the patterns. The self-reported crash data of drivers were used to verify the reliability of the score. The proposed method makes it possible to apply the G-G diagram to large-scale unlabeled driving data that are becoming increasingly prevalent in the context of ITS. With the proposed method, the numerous risky driving behaviors of the driver were decomposed into several risk components, which facilitated driving risk analysis. The spatio-temporal characteristics can be used to illustrate the potential cause of a driver's risky driving behavior. The results show that it is necessary to consider the relationship between the lateral and longitudinal accelerations to assess a driver's driving style since the magnitude of the longitudinal acceleration generally decreases when that of lateral acceleration increases. There is heterogeneity in drivers' risky driving behaviors. Risky acceleration and braking patterns were detected for all high-risk drivers and accounted for a significant part of the driving risk. The combination of lateral and longitudinal accelerations accounted for the majority of the driving risk for low-risk drivers. The developed performance score is reliable for measuring the driving risk of drivers, as crash-involved drivers were associated with lower performance scores. The analysis of the spatio-temporal context for two drivers shows that not all risky acceleration maneuvers are aggressive driving behaviors. The spatio-temporal characteristics can provide implicit factors regarding the risky driving behavior of drivers. Their intentions can be inferred from the context information.

Results of this study can be used to create a risk profile to provide driving feedback for each driver. Drivers can be trained to improve their driving behavior based on the feedback. This risk profile can also be used in the UBI scheme to determine the premium amount based on the risk level or performance score. Furthermore, the outcome can be used to enhance the benefits of ITS, particularly the intelligent vehicles. A personalized driving assistance system can be developed based on the results. The parameters of the system can be set according to the driver's driving risk component and the system can be set to assist the driver's driving in appropriate scenarios (i.e., individual behavioral hotspots). It has been shown that personalized driving assistance systems are more acceptable and user-friendly compared to regular ones [56]. Intelligent vehicles can also warn drivers before entering any individual behavioral hotspots, and a good driving plan can be prepared to help them avoid challenging circumstances.

ACKNOWLEDGMENT

This work was supported by a Grant-in-Aid for Scientific Research from the Takata Foundation in Japan and partially supported by JST COI under Grant No. JPMJCE1317.

AVAILABILITY OF DATA

The data used in this study is not available publicly because participants in this study did not give written consent for their data to be shared publicly.

REFERENCES

[1]F. Sagberg, B. P. Selpi, F. Giulio, and J. Engstr¨om, "A review of research on driving styles and road safety," Hum. Factors vol. 57 (7), pp. 1248–1275, 2015. https://doi.org/10.1177/0018720815591313.

[2]L. Eboli, G. Mazzulla, and G. Pungillo, "How to define the accident risk level of car drivers by combining objective and subjective measures of driving style," Transportation Research Part F: Traffic Psychology and Behavior, vol. 49, 2017, pp. 29–38.

[3]H. Singh and A Kathuria, "Profiling drivers to assess safe and eco-driving behavior–A systematic review of naturalistic driving studies," Accident Analysis & Prevention, vol. 161, 2021a, pp. 106349.

[4]S. Singh, "Critical reasons for crashes investigated in the national motor vehicle crash causation survey," Natl. Highw. Traffic Saf. Adm., 2018 March.

[5]S. Tanvir, R. T. Chase, and N. M. Roupahil, "Development and analysis of ecodriving metrics for naturalistic instrumented vehicles," J. Intell. Transp. Syst. vol. 25 (3), 2019, pp. 235–248. https://doi.org/10.1080/15472450.2019.1615486.

[6]M. Makridis, L. Leclercq, B. Ciuffo, G. Fontaras, and K. Mattas, "Formalizing the heterogeneity of the vehicle-driver system to reproduce traffic oscillations," Transportation Research Part C: Emerging Technologies, vol. 120, 2020, pp. 102803.

[7] Montanino, M., & Punzo, V. (2021). "On string stability of a mixed and heterogeneous traffic flow: A unifying modelling framework," Transportation Research Part B: Methodological, vol. 144, 2021, pp. 133-154.

[8] H. Singh and A. Kathuria, "Analyzing driver behavior under naturalistic driving conditions: A review," Accident Analysis & Prevention, vol. 150, 2021b, pp. 105908.

[9] R. Sangrar, J. Mun, M. Cammarata, L. E. Griffith, and L. Letts, and B. Vrkljan, "Older driver training programs: A systematic review of evidence aimed at improving behind-the-wheel performance," Journal of Safety Research, vol. 71, 2019, pp. 295–313.

[10] M. Rutty, L. Matthews, J. Andrey, and T. Del, "Eco-driver training within the city of Calgary's municipal fleet: Monitoring the impact," Transp. Res. Part D vol. 24 (2013), 2020, pp. 44–51. https://doi.org/10.1016/j.trd.2013.05.006.

[11]W. Wang, J. Xi, and D. Zhao, "Driving style analysis using primitive driving patterns with Bayesian nonparametric approaches," IEEE Transactions on Intelligent Transportation Systems, vol. 20(8), 2018, pp. 2986–2998.

[12]E. G. Mantouka and E. I. Vlahogianni, "Deep reinforcement learning for personalized driving recommendations to mitigate aggressiveness and riskiness: modeling and impact assessment," Transportation Research Part C: Emerging Technologies, vol. 142, p. 103770, 2022.

[13]M. Da Lio, F. Biral, and E. Bertolazzi, "Combining safety margins and user preferences into a driving criterion for optimal control-based computation of reference manoeuvres for an ADAS of the next generation," In Intelligent Vehicles Symposium. Las Vegas, USA, June 6–8 2005.

[14] M. Van Ly, S. Martin, and M. M. Trivedi, "Driver classification and driving style recognition using inertial sensors," 2013 IEEE Intelligent Vehicles Symposium (IV), 2013, pp. 1040–1045.

[15] J. Suarez, M. Makridis, A. Anesiadou, D. Komnos, B. Ciuffo, and G. Fontaras, "Benchmarking the driver acceleration impact on vehicle energy consumption and CO2 emissions," Transportation Research Part D: Transport and Environment, vol. 107, 2022, pp. 103282.

[16] M. Makridis, L. Leclercq, B. Ciuffo, G. Fontaras, and K. Mattas, "Formalizing the heterogeneity of the vehicle-driver system to reproduce traffic oscillations," Transportation Research Part C: Emerging Technologies, vol. 120, 2020, pp. 102803.

[17] J. W. Joubert, D. de Beer, and N. de Koker, "Combining accelerometer data and contextual variables to evaluate the risk of driver behavior," Transportation Research Part F: Traffic Psychology and Behavior, vol. 41, 2016, pp. 80–96.

[18] R. Vaiana, T. Iuele, V. Astarita, M. V. Caruso, A. Tassitani, C. Zaffino, and V. P. Giofre, "Driving behavior and traffic safety: An acceleration-based safety evaluation procedure for smartphones," Modern Applied Science, vol. 8, 2014, pp. 88–96.

[19] O. Derbel and R. Landry, Jr., "Driver behavior assessment based on the G-G diagram in the DVE system," IFAC-PapersOnLine, vol. 49(11), 2016, pp. 89–94.

[20] L. Eboli, G. Mazzulla, and G. Pungillo, "Combining speed and acceleration to define car users' safe or unsafe driving behavior,"

Transportation Research Part C: Emerging Technologies, vol. 68, 2016, pp. 113–125.
[21] M. N. Azadani and A. Boukerche, "Driving behavior analysis guidelines for intelligent transportation systems," IEEE Transactions on Intelligent Transportation Systems, 2021.
[22] S. Will, B. Metz, T. Hammer, M. Mörbe, M. Henzler, F. Harnischmacher, and G. Matschl, "Methodological considerations regarding motorcycle naturalistic riding investigations based on the use of gg diagrams for rider profile detection," Safety Science, vol. 129, 2020, pp. 104840.
[23] A. Cura, H. Küçük, E. Ergen, and İ. B. Öksüzoğlu, "Driver profiling using long short term memory (LSTM) and convolutional neural network (CNN) methods," IEEE Transactions on Intelligent Transportation Systems, vol. 22(10), 2020, pp. 6572–6582.
[24] A. E. Abdelrahman, H. S. Hassanein, and N. Abu-Ali, "Robust data-driven framework for driver behavior profiling using supervised machine learning," IEEE Transactions on Intelligent Transportation Systems, vol. 23(4), 2022, pp. 3336–3350.
[25] M. M. Bejani and M. Ghatee, "A context aware system for driving style evaluation by an ensemble learning on smartphone sensors data," Transportation Research Part C: Emerging Technologies, vol. 89, 2018, pp. 303–320.
[26] L. M. Bergasa, D. Almería, J. Almazán, J. J. Yebes, and R. & Arroyo, "Drivesafe: An app for alerting inattentive drivers and scoring driving behaviors," In Proceedings of IEEE Intelligent Vehicles Symposium, Dearborn, MI, USA, 08–11 June 2014, 240–245.
[27] A. B. Ellison, S. P. Greaves, and M. C. J Bliemer, "Driver behaviour profiles for road safety analysis," Accid. Anal. Prev. vol. 76, 2015, pp. 118–132. https://doi.org/10.1016/j. aap.2015.01.009.
[28] Y. Ma, W. Li, K. Tang, Z. Zhang, and S. Chen, "Driving style recognition and comparisons among driving tasks based on driver behavior in the online car-hailing industry," Accident Analysis & Prevention, vol. 154, 2021, pp. 106096.
[29] K. Fadhloun, H. Rakha, A. Loulizi, and A. Abdelkefi, A. "Vehicle dynamics model for estimating typical vehicle accelerations," Transportation research record, vol. 2491(1), 2015, pp. 61-71.
[30] M. A. Makridis, A Anesiadou, K. Mattas, G. Fontaras, and B Ciuffo, "Characterising driver heterogeneity within stochastic traffic simulation," Transportmetrica B: Transport Dynamics, 2022, pp. 1-19.
[31] M. A. Makridis and A. Kouvelas, "Adaptive physics-informed trajectory reconstruction exploiting driver behavior and car dynamics," Scientific Reports, vol. 13(1), 2023, pp. 1121.
[32] Y. Hisaoka, M. Yamamoto, and A. Okada, "Closed-loop analysis of vehicle behavior during braking in a turn," JSAE review, vol. 20(4), 1999, pp. 537-542.
[33] M. Siami, M. Naderpour, and J. A. Lu, "Mobile telematics pattern recognition framework for driving behavior extraction," IEEE Transactions on Intelligent Transportation Systems, vol. 22(3), 2020, pp. 1459–1472.
[34] Z. Constantinescu, C. Marinoiu, and M. Vladoiu, "Driving style analysis using data mining techniques," International Journal of Computers Communications & Control, vol. 5(5), 2010, pp. 654–663.
[35] E. G. Mantouka, E. N. Barmpounakis, and E. I. Vlahogianni, "Identifying driving safety profiles from smartphone data using unsupervised learning," Safety Science, vol. 119, 2019, pp. 84–90.
[36] J. Lee and K. Jang, "A framework for evaluating aggressive driving behaviors based on in-vehicle driving records," Transportation Research Part F: Traffic Psychology and Behaviour, vol. 65, 2019, pp. 610–619.
[37] D. A. Reynolds, "Gaussian mixture models," Encyclopedia of Biometrics, vol. 741, 2019, pp. 659–663.
[38] Z. Hong, Y. Chen, and Y. Wu, "A driver behavior assessment and recommendation system for connected vehicles to produce safer driving environments through a "follow the leader" approach," Accident Analysis & Prevention, vol, 139, 2020, pp. 105460.
[39] M. A. T. Figueiredo and A. K. Jain, "Unsupervised learning of finite mixture models," IEEE Transactions on Pattern Analysis and Machine Intelligence, vol. 24(3), 2002, pp. 381–396.
[40] B. Zhu, Y. Jiang, J. Zhao, R. He, N. Bian, and W. Deng, "Typical driving-style-oriented personalized adaptive cruise control design based on human driving data," Transportation Research Part C: Emerging Technologies, 100, 2019, 274–288.
[41] C. Ryan, F. Murphy, and M. Mullins, "Spatial risk modelling of behavioural hotspots: Risk-aware path planning for autonomous vehicles," Transportation Research Part A: Policy and Practice, vol. 134, 2020, pp. 152–163.
[42] E. Grimberg, A. Botzer, and O. Musicant, "Smartphones vs. in-vehicle data acquisition systems as tools for naturalistic driving studies: A comparative review," Safety science, vol. 131, 2020, pp. 104917.
[43] H. Chu et al., "A Review of Driving Style Recognition Methods From Short-Term and Long-Term Perspectives" in IEEE Transactions on Intelligent Vehicles, 2023, pp .
[44] G. Qi, J. Wu, Y. Zhou, Y. Du, Y. Jia, N. Hounsell, and N. A. Stanton, "Recognizing driving styles based on topic models," Transportation research part D: transport and environment, vol. 66, 2019, pp. 13-22.
[45] G. Castignani, T. Derrmann, R. Frank, and T. Engel, "Smartphone- based adaptive driving maneuver detection: A large-scale evaluation study," IEEE Transactions on Intelligent Transportation Systems, vol. 18(9), 2017, pp. 2330–2339.
[46] J. Wang, W. Xu, T. Fu, and R. Jiang, "Recognition of trip-based aggressive driving: A system integrated with gaussian mixture model structured of factor-analysis, and hierarchical clustering," IEEE Transactions on Intelligent Transportation Systems, 2022.
[47] V. Cohen-Addad, V. Kanade, F. Mallmann-Trenn, and C. Mathieu, "Hierarchical clustering: Objective functions and algorithms," J. ACM, vol. 66(4), 2019, pp. 378–397.
[48] J. H. Ward, Jr., "Hierarchical grouping to optimize an objective function," Journal of the American Statistical Association, vol. 58(301), 1963, pp. 236–244.
[49] P. Choudhary, A. Gupta, and N. R. Velaga, "Perceived risk vs actual driving performance during distracted driving: A comparative analysis of phone use and other secondary distractions," Transportation Research Part F: Traffic Psychology and Behavior, vol. 86, 2022, pp. 296–315.
[50] P.J. Rousseeuw, "Silhouettes: A graphical aid to the interpretation and validation of cluster analysis," J. Comput. Appl. Math. Vol. 20, 1987, pp. 53–65.
[51] G. J. McLachlan and S. Rathnayake, "On the number of components in a Gaussian mixture model," Wiley Interdisciplinary Reviews: Data Mining and Knowledge Discovery, 4vol. (5), 2014, pp. 341–355.
[52] J. Betz, A. Heilmeier, A. Wischnewski, T. Stahl, and M. Lienkamp, "Autonomous driving—A crash explained in detail," Applied Sciences, vol. 9(23), 2019, pp. 5126.
[53] G. Castignani, T. Derrmann, R. Frank, and T. Engel, "Driver behavior profiling using smartphones: A behavior profiling using smartphones," IEEE Intelligent Transportation Systems Magazine, vol. 7(1), 2015, pp. 91–102.
[54] P. Alrassy, A. W. Smyth, and J. Jang, "Driver behavior indices from large-scale fleet telematics data as surrogate safety measures," Accident Analysis & Prevention, vol. 179, 2023, p. 106879.
[55] V. Petraki, A. Ziakopoulos, and G. Yannis, "Combined impact of road and traffic characteristic on driver behavior using smartphone sensor data," Accident Analysis & Prevention, vol. 144, p. 105657, 2020.
[56] D. Yi, J. Su, C. Liu, M. Quddus, and W. H. Chen, "A machine learning based personalized system for driving state recognition," Transportation Research Part C: Emerging Technologies, vol. 105, 2019, pp. 241-261.
[57] T. H. Itkonen, J. Pekkanen, O. Lappi, I. Kosonen, T. Luttinen, and H. Summala, "Trade-off between jerk and time headway as an indicator of driving style," PloS one, vol. 12(10), 2017, e0185856.

Yuanfang Zhu has received the Master of Engineering in civil engineering from Nagoya University, Japan, in 2021. He is currently a PhD student of the department of civil and environmental engineering, Nagoya University, Japan. His research interest is on the study of driving behavior modelling and analysis, particularly the driving behavior of elderly people to help safe driving of the elderly.

Meilan Jiang has received the Master of Engineering in civil engineering from Tsinghua University, China, in 2000, and the Doctor of Engineering in transportation planning from Nagoya University, Japan, in 2003. She is currently an Associate Professor in the Institutes of Innovation for Future Society, Nagoya University, Japan. Her research interests include traffic safety, travel behavior analysis, mobility sharing systems, mobility values, intelligent transport systems, et al.

Toshiyuki Yamamoto received the Doctor of Engineering on transportation planning from Kyoto University, Japan, in 2000. He is currently a Professor with the Institute of Materials and Systems for Sustainability, Nagoya University, Japan. His research interests include vehicle ownership and use, vehicle sharing systems, travel behaviour analysis, time use and activity-based analysis, intelligent transport systems, and traffic safety.

Naikan Ding received a Ph.D. from Wuhan University of Technology (WUT), Wuhan, China, in 2017. He is an Associate Professor at the Intelligent Transportation Systems Research Center (ITSC), WUT, and was a Postdoctoral Researcher at the Department of Civil Engineering, Nagoya University. His research interests include traffic safety, driving behavior, human factors, and connected automated vehicles.

Hiroko Shinkai has been a training instructor in a driving school since 1993, and a practical instructor in the Training Center of Japan Safe Driving Center from 2005 to 2008. Since 2008, she has been a member of driving instructor of the Aichi Prefecture Federation of Authorized Drivers School Associations and assumed the position of a board member of the federation since 2017. She is currently a researcher of the Institute of Innovation for Future Society in Nagoya University since 2020.

Hirofumi Aoki (Member, IEEE) received M.S. and Ph.D. from Tokyo Institute of Technology. After working as a postdoctoral fellow at MIT and the National Space Biomedical Research Institute, he joined Toyota Motor Corporation. Since 2014, he has been a professor at the Institutes of Innovation for Future Society, Nagoya University. Dr. Aoki is a board member of the Society of Automotive Engineers of Japan and Japan Human Factors and Ergonomics Society.

Kan Shimazaki born in Tokyo, JAPAN in February 1976. Withdrawal with credits by Graduate School of Human Sciences, Waseda University. Ph.D. (Human Sciences), Tokyo, JAPAN, 2009. 2008 joined Faculty of human sciences, Waseda Univ. as Research associate, 2011- Assistant Professor of Faculty of human sciences, Waseda Univ., 2015- Associated Research Fellow of National Institute of Earth Science and Disaster Resilience, 2019- Associate Professor of Institute of Innovation for Future Society, Nagoya University, 2022- Associate Professor of Biology-Oriented Science and Technology, Kindai University. His best-known book is A “Study of Anxiety”, published by Kobunsha. He is a member of The Japanese Association of Traffic Psychology (JATP), The Japanese Psychological Association (JPA), Japan Ergonomics Society (JES) and other societies. His major is psychology and focuses on increasing people's safe behaviors and reducing risks in society.